Hindawi
International Journal of Chemical Engineering
Volume 2022, Article ID 7119336, 10 pages
https://doi.org/10.1155/2022/7119336

Research Article

Insights into the Estimation of the Enhanced Thermal Conductivity of Phase Change Material-Containing Oxide Nanoparticles using Gaussian Process Regression Method

Tzu-Chia Chen,[1] **Hasan Sh. Majdi**,[2] **Aras Masood Ismael**,[3] **Jamshid Pouresmi**,[4] **Danial Ahangari**,[5] **and Saja Mohammed Noori**[6]

[1]*Department of Industrial Engineering and Management, Ming Chi University of Technology, New Taipei City 24301, Taiwan*
[2]*Al- Mustaqbal University College, Department of Chemical Engineering and Petroleum Industries, Hilla, Iraq*
[3]*Information Technology Department, Technical College of Informatics, Sulaimani Polytechnic University, Sulaymaniyah, Iraq*
[4]*Department of Instrumentation and Industrial Automation, Ahwaz Faculty of Petroleum Engineering, Petroleum University of Technology, Ahwaz, Iran*
[5]*Department of Geology, Faculty of Earth Sciences, S. Chamran University of Ahwaz, Ahwaz, Iran*
[6]*Department of Computer Network, College of Engineering and Computer Science, Lebanese French University, Kurdistan Region, Erbil, Iraq*

Correspondence should be addressed to Jamshid Pouresmi; jamshid.pouresmi@afp.put.ac.ir

Received 2 April 2022; Revised 1 May 2022; Accepted 6 May 2022; Published 9 June 2022

Academic Editor: Alireza Baghban

Thermal conductivity (TC) of a phase change material (PCM) may be enhanced by distributing nanostructured materials (NSMs) termed nano-PCM. It is critical to accurately estimate the TC of nano-PCM to assess heat transfer during phase transition processes, namely, solidification and melting. Here, we propose Gaussian process regression (GPR) strategies involving four various kernel functions (KFs) (including exponential (E), squared exponential (SE), rational quadratic (RQ), and matern (M)) to predict TC of n-octadecane as a PCM. The accessible computational techniques indicate the accuracy of our proposed GPR model compared to the previously proposed methods. In this research, the foremost forecasting strategy has been considered as a GPR method. This model consists of the matern KF whose R^2 values of training and testing phases are 1 and 1, respectively. In the following, a sensitivity analysis (SA) is used to explore the effectiveness of variables in terms of outputs and shows that the temperature (T) of nanofluid (NF) is the most efficient input parameter. The work describes the physical properties of NFs and the parameters that should be determined to optimize their efficiency.

1. Introduction

PCMs are extensively utilized in thermal storage devices to store heat [1]. They may be categorized chemically as organic PCMs (fatty acids and paraffin), inorganic PCMs (salt hydrates and metallic), or eutectics PCMs [2]. Though PCMs exhibit higher latent fusion heat at relatively constant T, they have a relatively poor TC [3]. This has a remarkable and considerable effect on the pace of PC [4, 5]. To improve the thermal storage of PCMs, their thermal conductance must be increased. As a result, many improvement techniques have been suggested, including incorporating highly thermally conductive materials, including metallic and graphene porous foams [6–9] into the PCM, microencapsulation of the PCM [10, 11], high-TC fins [12], and integrated heat pipes PCM [13].

High-TC NSMs have been developed and marketed during the last several decades due to nanotechnology advancements. These nanostructures are made of a variety of materials, including metallic, carbon-based, and nonmetallic compounds [14]. NFs are a new category of heat transfer fluids made via incorporating nanoscale components into a

base fluid [15]. Among the alluring properties of NFs is the increased TC as opposed to the base fluid. The concept of enhancing the NFs' TC may be used to introduce PCMs with scattered NSMs that had increased TC compared to the basic PCMs [16]. In contrast to stationary enhancer structures, nanomaterials can retain the PCM's fluidity in the liquid state and prevent contact conductance issues; furthermore, nano-PCMs would be recyclable [16]. Numerous researchers have performed significant studies on the increased TC of PCMs incorporating various nanomaterials, including oxide nanoparticles (NPs) [17–19], carbon nanomaterials [20–22], and metallic NPs [23, 24].

Along with standard measures of the thermophysical characteristics of nano-PCMs, several academics have lately proposed various experimental studies to estimate these parameters [20, 25, 26]. Algorithms for machine learning (ML), such as artificial neural networks (ANNs), are founded on human neurons. These techniques have been widely employed in the last few years to forecast the thermophysical characteristics of new materials, particularly NFs [27]. Toghraie et al. [28] investigated the dynamic viscosity (μ) of an EG/AG NF. Ahmadi et al. [29] used the ANN intelligent technique to determine the dynamic μ of a SiO_2/EG-H_2O NF. Hemmat Esfe et al. [30], using an ANN, predicted the μ of a MWCNTs-ZnO/5W50 nanolubricant under various shear stresses, Ts, and volume concentrations. Chen et al. [31] used an ANN to determine the μ of MWCNTs-TiO_2/SAE50 hybrid NFs at various shear rates, volume fractions (VFs), and Ts. Hemmati-Sarapardeh et al. [32] have published a paper focused on intelligent techniques for the prediction of the NFs' TC. Rostamian et al. [33] used experimental data, ANNs, and nonlinear regression method to determine the TC of Cu-SWCNTs/EG hybrid NFs at various VFs and Ts. Shahsavar et al. [34] used oleic acid as a surfactant to investigate an alumina-liquid paraffin NF's μ and TC. Safaei et al. [35] used an ANN to predict the increased TC of ZnO/TiO_2 in ethylene glycol as a hybrid NF. The authors trained the ANNs using experimental data. Using a database containing 715 experimental data, Adun and his colleagues [36] estimated the TC of hybrid NFs. They accomplished this by developing support vector regression and multiple linear regression models. Hemmat Esfe et al. [37] utilized ANNs and response surface methodology for predicting the TC of TiO_2 in H_2O NFs. Peng et al. [38] used the ANN technique and a suggested correlation to model the TC of an alumina/Cu-ethylene glycol NF. Li et al. [39] presented novel correlations and an optimum ANN for measuring μ and TC of alumina-ethylene glycol NFs based on several sets of experiments. VFs and Ts of NPs are input to a feedforward ANN. Çolak [40] studied the TC of ZrO_2-H_2O NFs at a range of concentrations and Ts. Barewar et al. [41] examined the thermophysical characteristics of Ag/ZnO-EG NFs with VFs ranging from 0.05 to 0.2 vol. % to ZnO-EG NFs. Ghazvini et al. [42] presented a two-layered ANN for determining the TC ratio of a $CuFe_2O_4$-H_2O NF based on experimentally determined thermal conductivities. He and his colleagues [43] used ANNs and correlation methods to approximate the TC of a ZnO/Ag-H_2O hybrid NF. The authors discovered that the most precise model using an ANN model combined with the Levenberg–Marquardt method. Pare and Ghosh [44] studied the TC of Al_2O_3, CuO, and ZrO_2 in H_2O NFs. The TC of NFs was determined at weight concentrations ranging from 0.02 to 2% and Ts ranging from 20 to 90°C. Rostami et al. [45] used curve fitting and ANNs to estimate the TC ratio of graphene oxide and copper oxide antifreeze NF.

The purpose of this research is to expand our understanding in a variety of ways. To begin, while the TC of NFs has been modeled using ANN, to the authors' information, GPR methods for projecting the TC of nano-PCMs had not been investigated. Secondly, since experimental TC measurements of different solid-liquid nano-PCMs are costly and time-consuming, GPR may be employed to correctly estimate the TC of nano-PCMs. To train these models, 122 experimental data from previous research are examined, with Ts ranging from 5°C to 60°C and mass fractions of NPs ranging from 0.5 to 12 wt. % [14, 25, 26, 46]. We used three quarters of this data in the model making stage and the rest in the model testing stage. Using this data, models with four various function kernels are developed and then using different statistical parameters, the accuracy of these models is examined and the best model to predict the target parameter is identified.

2. Methodology (GPR Model)

We follow a nonparametric approach, to model various inconsistent complex systems [47, 48]. In fact, we want to use one of the benefits of this method which is the flexibility of its algorithm to describe the uncertainty sources making it most attractive to researchers following prediction issues through that [49]. It is noted that the uncertainty sources are detected by GPR models [50]. As an instance, these models distribute the values predicted rather than only a predicted one. In addition, this model can have the capability to add characteristics and instruction on forms of models by employing different KFs manually. So, a covariance function (CovF), $k(x.x')$, and mean function, $m(x)$, are used to model time series as follows [51–53]:

$$y = f(x) \sim N(m(x), k(x, x')), \tag{1}$$

where output and input are depicted by y and x for training, respectively. Also, $f(x)$ describes the hidden variable of this algorithm [54]. It is popular to select the mean function as zero. CovF function is used to show the similarity between input variables. Because similar inputs may make similar outputs that are not useful for our database. The KFs of this study are described as follows [55, 56]:

Exponential

$$k(x, x') = \theta_1^2 \exp\left(\frac{-r}{\theta_2}\right), \tag{2}$$

$$r = \sqrt{(x, x')^T (x - x')}. \tag{3}$$

Squared exponential

$$k(x,x') = \theta_1^2 \exp\left(\frac{d^2}{2\theta_2^2}\right), \tag{4}$$

Where, θ_1 and θ_2 are the hyperparameters and must be optimized. Also, d is the Euclidean distance of x and x'.

Matern

$$k(x,x') = \frac{1}{\Gamma(v)2^{v-1}}\left(\frac{\sqrt{2vr}}{l}\right)^{v} k_v\left(\frac{\sqrt{2vr}}{l}\right). \tag{5}$$

Where the modified Bessel function is shown by K_v, and a positive parameter by v [57].

Rational quadratic

$$k(x,x') = \theta_1^2\left(1 + \frac{r^2}{2\propto\theta_2^2}\right), \tag{6}$$

where a covariance positive parameter is shown by α.

Before training the algorithm, the negative log marginalized likelihood (NLML) must be minimized and this is done by hyperparameters of KFs as follows [58]:

$$\begin{aligned}\text{NLML} = -\log(p(y|x,\theta)) &= -\frac{1}{2}\log\left|k + \sigma_n^2 I\right| \\ &\quad -\frac{1}{2}y^T\left(k + \sigma_n^2 I\right)^{-1} y - \frac{n}{2}\log(2\pi).\end{aligned} \tag{7}$$

This is an optimization process that must reach the minimum of θ. This process is explained as follows:

$$\widehat{\theta} = \arg\min -\log(p(y \mid x,\theta)). \tag{8}$$

During this process, NLML is minimized by optimization methods known as off-the-shelf methods. These methods utilize a convex function. Then, the testing phase is done to predict distribution as follows [59]:

$$\begin{aligned} &f_*|x,y,x_* \sim N\left(\overline{f*}, \operatorname{cov}(f_*)\right), \\ &\overline{f}_* = m(x,x_*) + K(x,x_*)\left(K(x,x) + \sigma_n^2 I\right)^{-1}(y - m(x)), \\ &\operatorname{cov}\left(\overline{f}_*\right) = K(x_*,x_*) - K(x_*,x)\left(K(x,x) + \sigma_n^2 I\right)^{-1} K(x,x_*), \end{aligned} \tag{9}$$

where $\overline{f*}$ and $\operatorname{cov}(\overline{f*})$ are the prediction results and prediction uncertainty, respectively. The average GPR distribution is linearly when $m(x) = 0$. In this case, this distribution is specified as a linear function of y used for training (see equation (10)) and defined as follows:

$$\overline{f}_* = K(x,x_*)\left(K(x,x) + \sigma_n^2 I\right)^{-1} y = W_{\text{GPRY}}, \tag{10}$$

where W_{GPR} is the weighting matrix.

3. Evaluating the Accuracy of the Gathered Databank

Here, outlier data are considered as data points. They have various behaviors compared to other data. These outlier data return data to the faults that occurred in the experimental method. These data result in false estimations of our proposed models. So, to improve the efficiency and integrity of our models, we must identify these kinds of data points. We can use the leverage method to enhance the databank quality. This method identifies the outlier data points by a Hat matrix defined as the following [60, 61]:

$$H = U\left(U^T U\right)^{-1} U^T, \tag{11}$$

where U refers to a $i * j$ dimensional matrix. The i and j show the number of model parameters and training points, respectively. To test this process, a critical leverage limit is considered as a parameter to identify the outlier data from others. This limit is defined as the following [62–64]:

$$H^* = \frac{3(j+1)}{i}. \tag{12}$$

Afterward, William's plot is used to evaluate the authenticity of the TC databank. As you see, the standard residuals are shown against the Hat values in Figure 1. In Figure 1, to define a reliable zone to use the dataset, a bounded area is considered between the critical limitations of leverage and standard residuals of −3 to 3. Then, William's plot is used to show the reliability of resulted TC data points. The value of outlier data for M, SE, E, and RQ models, was obtained 2, 3, 1, and 0, respectively. So, they are appropriate to test and train models.

4. Results and Discussion

4.1. SA. It is noted that researchers and engineers always track the way to identify the impact of input numbers on the TC to suggest an accurate model. So, a SA is the best way to achieve this goal. In this regard, they follow the relevancy factor, r, for every input variable as follows [65–67]:

$$r = \frac{\sum_{i=1}^{n}\left(X_{k,i} - \overline{X}_k\right)\left(Y_i - \overline{Y}\right)}{\sqrt{\sum_{i=1}^{n}\left(X_{k,i} - \overline{X}_k\right)^2 \sum_{i=1}^{n}\left(Y_i - \overline{Y}\right)^2}}, \tag{13}$$

where $X_{k,i}$ and Y_i are the input and output, respectively. $\overline{X_k}$ and $\overline{Y}$ are means of inputs and outputs, respectively.

The impact of every parameter on the TC is shown in Figure 2. Here, when the absolute value, r, of an input number increases, it influences on the TC more and conversely. Additionally, here the positive value depicts that every input variable has a direct relationship with TC. Moreover, the results show that Ts with positive r values, e.g., 0.98, are the most efficient variables to detect the TC.

4.2. Modeling Results. In this part, to explore the fulfillment of suggested models, many more attempts have been performed to predict the TC. Here, the assessment of the

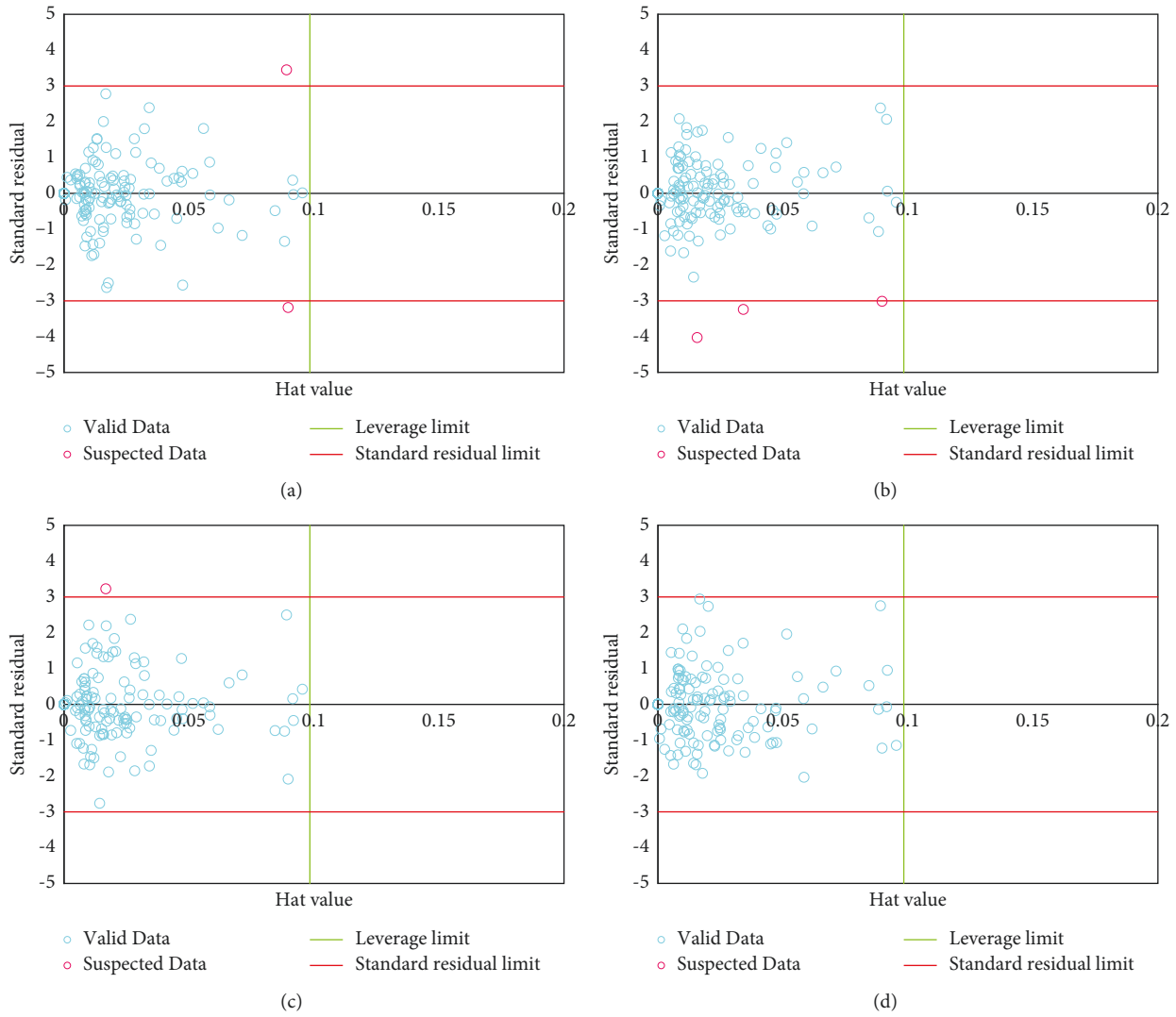

Figure 1: Detection of suspected data points using Hat analysis for models: (a) M, (b) E, (c) SE, and (d) RQ.

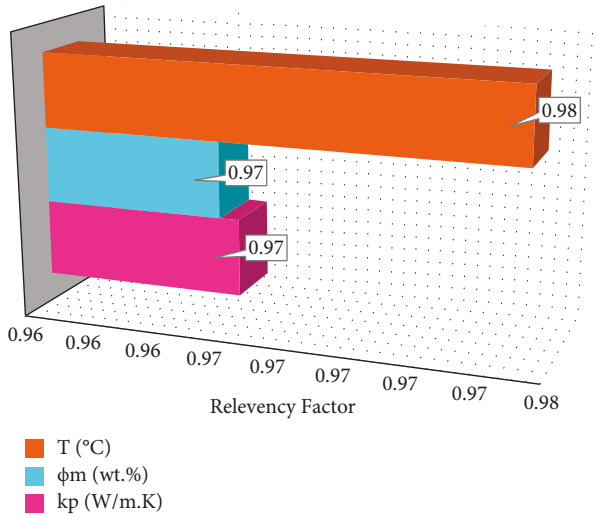

Figure 2: SA on the input parameters using relevancy factor for models: (a) M, (b) E, (c) SE, and (d) RQ.

performance of our models is conducted in two main ways employing graphical comparisons and matching parameters. To find out a match between the actual and predicted databank, the matching parameters have been utilized [68].

Table 1 reports the statistical parameters calculated for testing, training, and the whole dataset. You can see in this table that GPR models with RQ, E, M, and SE kernel functions have R^2 values of 0.999, 1, 1, and 0.999, respectively. In addition, lower values of other parameters including STD, MSE, MRE, and RMSE during the training phase show that they have had acceptable precision. In particular, this acceptable value is very important regardless of the model performance for estimating unseen TC points.

Figure 3 compares the experimental and predicted TC values of these models simultaneously. In the GPR models, there is a superior agreement between various GPR models and real TC.

Here, the experimental TC of all proposed models is exactly covered by the estimated TC. So, these models have

Table 1: Determining statistical parameters in different phases for models (a) M, (b) E, (c) SE, and (d) RQ.

Model	Set	R^2	MRE (%)	MSE	RMSE	STD
M	Train	1.000	0.610	$2.77298E-06$	0.0017	0.0011
	Test	1.000	0.465	$1.0165E-06$	0.0010	0.0006
	Total	1.000	0.574	$2.34106E-06$	0.0010	0.0010
E	Train	0.999	0.732	$6.37106E-06$	0.0025	0.0018
	Test	1.000	0.639	$4.38691E-06$	0.0021	0.0015
	Total	1.000	0.709	$5.88315E-06$	0.0021	0.0017
SE	Train	0.999	0.847	$6.65673E-06$	0.0026	0.0018
	Test	0.999	0.998	$7.82742E-06$	0.0028	0.0019
	Total	0.999	0.884	$6.94461E-06$	0.0028	0.0018
RQ	Train	0.999	1.078	$1.11893E-05$	0.0033	0.0022
	Test	0.999	0.898	$7.14543E-06$	0.0027	0.0018
	Total	0.999	1.034	$1.01949E-05$	0.0027	0.0021

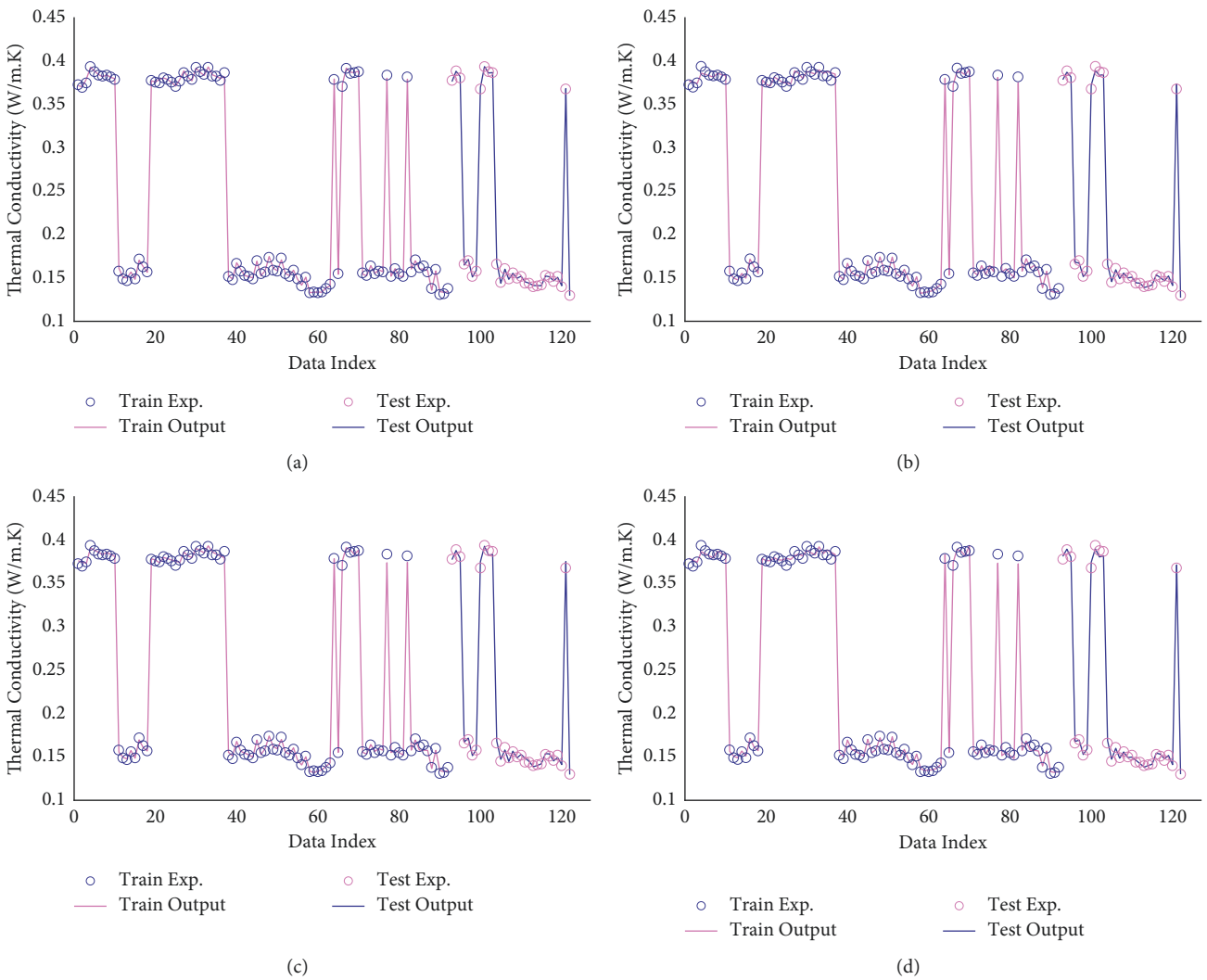

Figure 3: Visual and simultaneous comparison of actual and modeled output data using various KFs: (a) M, (b) E, (c) SE, and (d) RQ.

the reliability to perform and predict TC. In the following, Figure 4 depicts the cross plots of 4 GPR proposed models. They illustrate that the whole estimated TC is placed in its real values. We see their fitting lines and the bisector line of the first quarter have near similarity. Generally, the bisector line is used to measure the precision of the proposed models. Precision is higher when the data are very close to the 45°line.

Next, Figure 5 shows the relative deviations (RDs) between predicted TC and real values for all suggested models. In this study, M and KF have absolute deviation points less

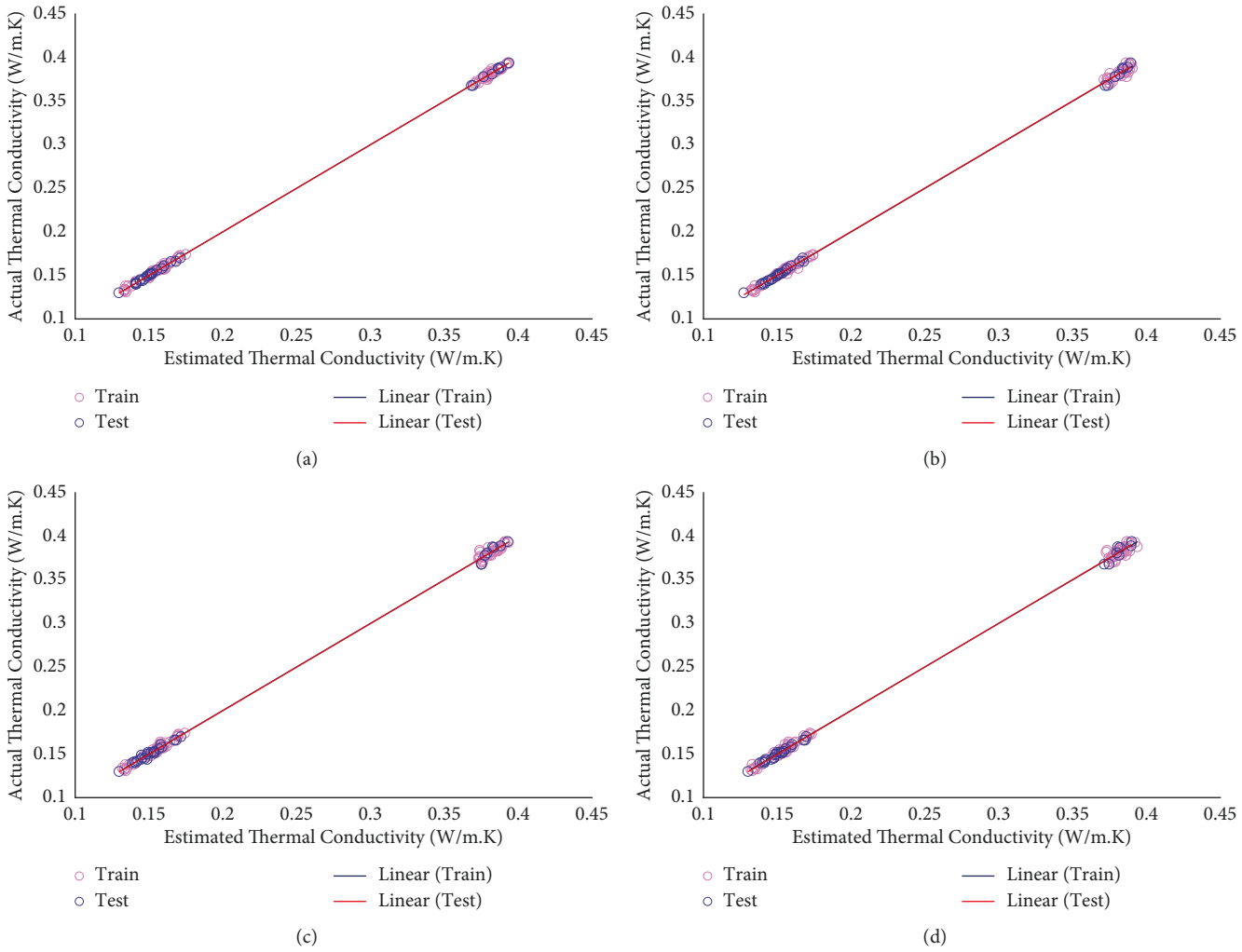

Figure 4: Cross plot analysis to determine the accuracy of different models in predicting target values using various KFs: (a) M, (b) E, (c) SE, and (d) RQ.

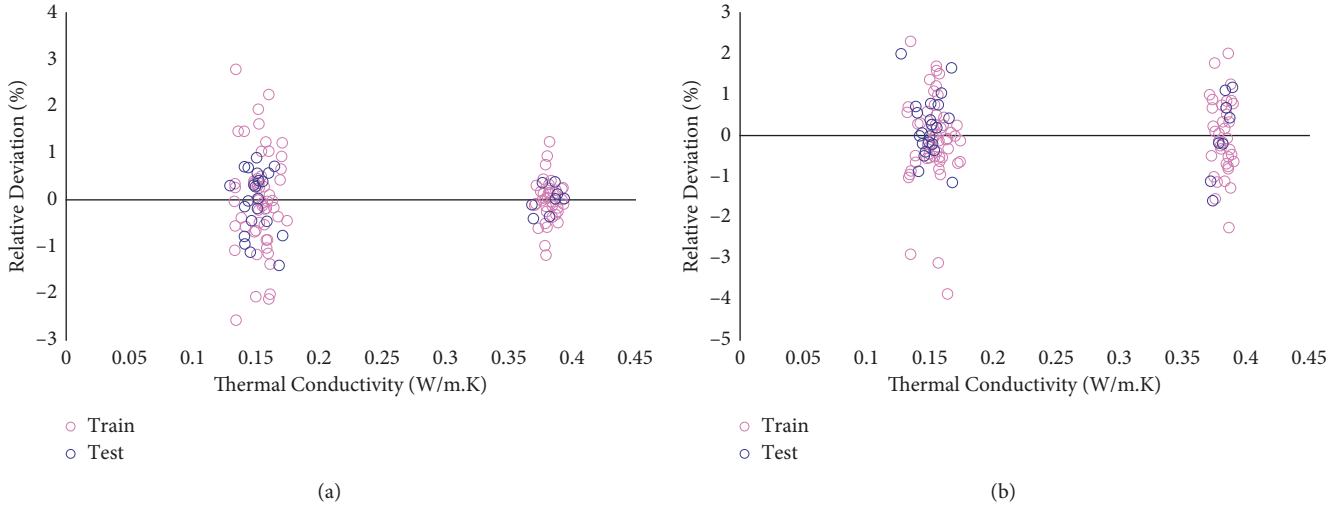

Figure 5: Continued.

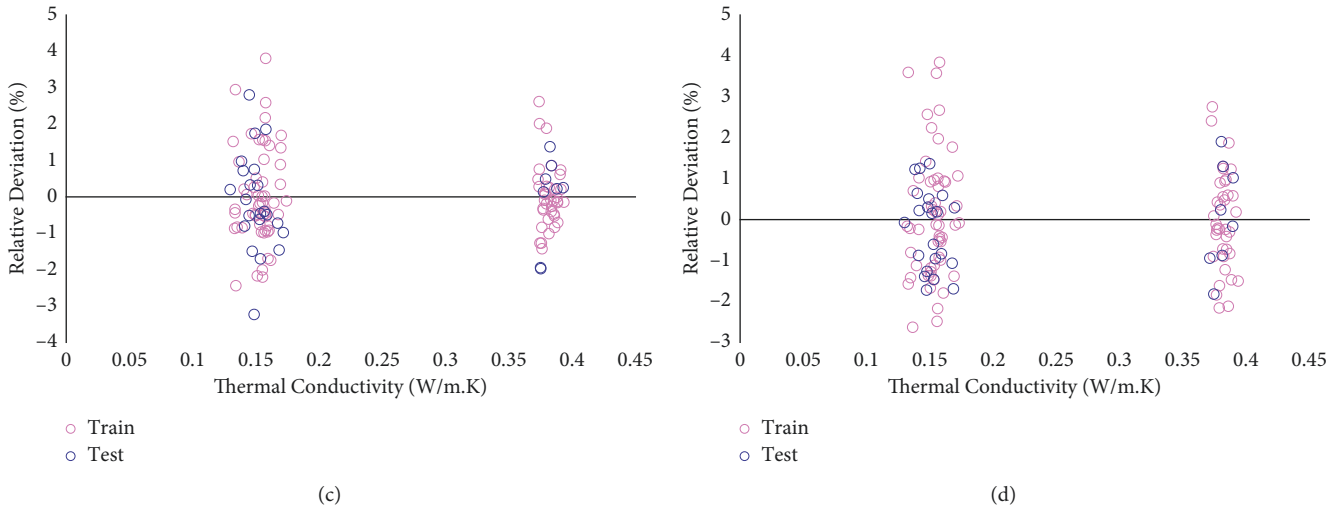

Figure 5: RD analysis to determine the accuracy of different models using various KFs: (a) M, (b) E, (c) SE, and (d) RQ.

than 3%, whereas various KFs of RQ, SE, and E have less than 4%.

5. Conclusions

In this research, we reach a high-degree match between real and predicted TC numbers with the help of evaluation of our suggested models and the collected databank. Our visual and mathematical comparisons show that our GPR models have an excellent capability to determine the enhanced TC of PCM-containing oxide NPs. Moreover, the SA illustrates that there is a direct relationship between all input parameters and TC. This study is a road map for the engineering communities to forecast the behavior of the heat exchanger and that of refrigeration systems even though having little knowledge about artificial intelligence techniques and nanoscience.

Data Availability

The references to experimental data used to support the findings of this study are included within the article.

Conflicts of Interest

The authors declare that they have no conflicts of interest.

References

[1] L. Liu, D. Su, Y. Tang, and G. Fang, "Thermal conductivity enhancement of phase change materials for thermal energy storage: a review," *Renewable and Sustainable Energy Reviews*, vol. 62, pp. 305–317, 2016.

[2] Z. A. Qureshi, H. M. Ali, and S. Khushnood, "Recent advances on thermal conductivity enhancement of phase change materials for energy storage system: a review," *International Journal of Heat and Mass Transfer*, vol. 127, pp. 838–856, 2018.

[3] Y.-D. Liu, Y. G. Zhou, M. W. Tong, and X. S. Zhou, "Experimental study of thermal conductivity and phase change performance of nanofluids PCMs," *Microfluidics and Nanofluidics*, vol. 7, no. 4, pp. 579–584, 2009.

[4] Y. Lin, Y. Jia, G. Alva, and G. Fang, "Review on thermal conductivity enhancement, thermal properties and applications of phase change materials in thermal energy storage," *Renewable and Sustainable Energy Reviews*, vol. 82, pp. 2730–2742, 2018.

[5] M. Arıcı, E. Tutuncu, C. Yildiz, and D. Li, "Enhancement of PCM melting rate via internal fin and nanoparticles," *International Journal of Heat and Mass Transfer*, vol. 156, Article ID 119845, 2020.

[6] V. Mayilvelnathan and A. Valan Arasu, "Experimental investigation on thermal behavior of graphene dispersed erythritol PCM in a shell and helical tube latent energy storage system," *International Journal of Thermal Sciences*, vol. 155, Article ID 106446, 2020.

[7] Y. Lin, R. Cong, Y. Chen, and G. Fang, "Thermal properties and characterization of palmitic acid/nano silicon dioxide/graphene nanoplatelet for thermal energy storage," *International Journal of Energy Research*, vol. 44, no. 7, pp. 5621–5633, 2020.

[8] R. M. Lazzarin, S. Mancin, M. Noro, and G. Righetti, "Hybrid PCM—aluminium foams' thermal storages: an experimental study," *International Journal of Low Carbon Technologies*, vol. 13, no. 3, pp. 286–291, 2018.

[9] Y. Huo, Y. Guo, and Z. Rao, "Investigation on the thermal performance of phase change material/porous medium-based battery thermal management in pore scale," *International Journal of Energy Research*, vol. 43, no. 2, pp. 767–778, 2019.

[10] B. Srinivasaraonaik, L. P. Singh, I. Tyagi, A. Rawat, and S. Sinha, "Microencapsulation of a eutectic PCM using in situ polymerization technique for thermal energy storage," *International Journal of Energy Research*, vol. 44, no. 5, pp. 3854–3864, 2020.

[11] X. Huang, C. Zhu, Y. Lin, and G. Fang, "Thermal properties and applications of microencapsulated PCM for thermal energy storage: a review," *Applied Thermal Engineering*, vol. 147, pp. 841–855, 2019.

[12] D. S. Mehta, B. Vaghela, M. K. Rathod, and J. Banerjee, "Enrichment of heat transfer in a latent heat storage unit using longitudinal fins," *Heat Transfer*, vol. 49, no. 5, pp. 2659–2685, 2020.

[13] S. Motahar and R. Khodabandeh, "Experimental study on the melting and solidification of a phase change material

enhanced by heat pipe," *International Communications in Heat and Mass Transfer*, vol. 73, pp. 1–6, 2016.

[14] S. Motahar, N. Nikkam, A. A. Alemrajabi, R. Khodabandeh, M. S. Toprak, and M. Muhammed, "A novel phase change material containing mesoporous silica nanoparticles for thermal storage: a study on thermal conductivity and viscosity," *International Communications in Heat and Mass Transfer*, vol. 56, pp. 114–120, 2014.

[15] M. H. Ahmadi, A. Mirlohi, M. Alhuyi Nazari, and R. Ghasempour, "A review of thermal conductivity of various nanofluids," *Journal of Molecular Liquids*, vol. 265, pp. 181–188, 2018.

[16] J. Khodadadi, L. Fan, and H. Babaei, "Thermal conductivity enhancement of nanostructure-based colloidal suspensions utilized as phase change materials for thermal energy storage: a review," *Renewable and Sustainable Energy Reviews*, vol. 24, pp. 418–444, 2013.

[17] H. E. Abdelrahman, M. Wahba, H. Refaey, M. Moawad, and N. Berbish, "Performance enhancement of photovoltaic cells by changing configuration and using PCM (RT35HC) with nanoparticles Al2O3," *Solar Energy*, vol. 177, pp. 665–671, 2019.

[18] M. Sheikholeslami, A. Ghasemi, Z. Li, A. Shafee, and S. Saleem, "Influence of CuO nanoparticles on heat transfer behavior of PCM in solidification process considering radiative source term," *International Journal of Heat and Mass Transfer*, vol. 126, pp. 1252–1264, 2018.

[19] G. Zhang, Z. Wang, D. Li, Y. Wu, and M. Arici, "Seasonal thermal performance analysis of glazed window filled with paraffin including various nanoparticles," *International Journal of Energy Research*, vol. 44, no. 4, pp. 3008–3019, 2020.

[20] S. Motahar, A. A. Alemrajabi, and R. Khodabandeh, "Enhanced thermal conductivity of n-octadecane containing carbon-based nanomaterials," *Heat and Mass Transfer*, vol. 52, no. 8, pp. 1621–1631, 2016.

[21] Y. Qu, S. Wang, D. Zhou, and Y. Tian, "Experimental study on thermal conductivity of paraffin-based shape-stabilized phase change material with hybrid carbon nano-additives," *Renewable Energy*, vol. 146, pp. 2637–2645, 2020.

[22] R. I. Rabady and D. S. Malkawi, "Thermal conductivity enhancement of sodium thiosulfate pentahydrate by adding carbon nano-tubes/graphite nano-particles," *Journal of Energy Storage*, vol. 27, Article ID 101166, 2020.

[23] I.-H. Kim, H. W. Sim, H. H. Hong, D. W. Kim, W. Lee, and D. K. Lee, "Effect of filler size on thermal properties of paraffin/silver nanoparticle composites," *Korean Journal of Chemical Engineering*, vol. 36, no. 6, pp. 1004–1012, 2019.

[24] N. Xie, J. Niu, X. Gao, Y. Fang, and Z. Zhang, "Fabrication and characterization of electrospun fatty acid form-stable phase change materials in the presence of copper nanoparticles," *International Journal of Energy Research*, vol. 44, no. 11, pp. 8567–8577, 2020.

[25] V. B. Águila, D. A. Vasco, P. Galvez, and P. A. Zapata, "Effect of temperature and CuO-nanoparticle concentration on the thermal conductivity and viscosity of an organic phase-change material," *International Journal of Heat and Mass Transfer*, vol. 120, pp. 1009–1019, 2018.

[26] S. Motahar, N. Nikkam, A. A. Alemrajabi, R. Khodabandeh, M. S. Toprak, and M. Muhammed, "Experimental investigation on thermal and rheological properties of n-octadecane with dispersed TiO2 nanoparticles," *International Communications in Heat and Mass Transfer*, vol. 59, pp. 68–74, 2014.

[27] S. Motahar and S. Sadri, "Applying artificial neural networks to predict the enhanced thermal conductivity of a phase change material with dispersed oxide nanoparticles," *International Journal of Energy Research*, vol. 45, no. 10, pp. 15092–15109, 2021.

[28] D. Toghraie, N. Sina, N. A. Jolfaei, M. Hajian, and M. Afrand, "Designing an Artificial Neural Network (ANN) to predict the viscosity of Silver/Ethylene glycol nanofluid at different temperatures and volume fraction of nanoparticles," *Physica A: Statistical Mechanics and Its Applications*, vol. 534, Article ID 122142, 2019.

[29] M. H. Ahmadi, M. Sadeghzadeh, H. Maddah, A. Solouk, R. Kumar, and Kw Chau, "Precise smart model for estimating dynamic viscosity of SiO2/ethylene glycol–water nanofluid," *Engineering Applications of Computational Fluid Mechanics*, vol. 13, no. 1, pp. 1095–1105, 2019.

[30] M. Hemmat Esfe, M. Goodarzi, M. Reiszadeh, and M. Afrand, "Evaluation of MWCNTs-ZnO/5W50 nanolubricant by design of an artificial neural network for predicting viscosity and its optimization," *Journal of Molecular Liquids*, vol. 277, pp. 921–931, 2019.

[31] Z. Chen, A. Z. Ashkezari, and I. Tlili, "Applying artificial neural network and curve fitting method to predict the viscosity of SAE50/MWCNTs-TiO2 hybrid nanolubricant," *Physica A: Statistical Mechanics and its Applications*, vol. 549, Article ID 123946, 2020.

[32] A. Hemmati-Sarapardeh, A. Varamesh, M. Nait Amar, M. M. Husein, and M. Dong, "On the evaluation of thermal conductivity of nanofluids using advanced intelligent models," *International Communications in Heat and Mass Transfer*, vol. 118, Article ID 104825, 2020.

[33] S. H. Rostamian, M. Biglari, S. Saedodin, and M. Hemmat Esfe, "An inspection of thermal conductivity of CuO-SWCNTs hybrid nanofluid versus temperature and concentration using experimental data, ANN modeling and new correlation," *Journal of Molecular Liquids*, vol. 231, pp. 364–369, 2017.

[34] A. Shahsavar, S. Khanmohammadi, D. Toghraie, and H. Salihepour, "Experimental investigation and develop ANNs by introducing the suitable architectures and training algorithms supported by sensitivity analysis: measure thermal conductivity and viscosity for liquid paraffin based nanofluid containing Al2O3 nanoparticles," *Journal of Molecular Liquids*, vol. 276, pp. 850–860, 2019.

[35] M. R. Safaei, A. Hajizadeh, M. Afrand, C. Qi, H. Yarmand, and N. W. B. M. Zulkifli, "Evaluating the effect of temperature and concentration on the thermal conductivity of ZnO-TiO2/EG hybrid nanofluid using artificial neural network and curve fitting on experimental data," *Physica A: Statistical Mechanics and Its Applications*, vol. 519, pp. 209–216, 2019.

[36] H. Adun, I. Wole-Osho, E. C. Okonkwo, O. Bamisile, M. Dagbasi, and S. Abbasoglu, "A neural network-based predictive model for the thermal conductivity of hybrid nanofluids," *International Communications in Heat and Mass Transfer*, vol. 119, Article ID 104930, 2020.

[37] M. Hemmat Esfe, S. M. Motallebi, and M. Bahiraei, "Employing response surface methodology and neural network to accurately model thermal conductivity of TiO2–water nanofluid using experimental data," *Chinese Journal of Physics*, vol. 70, pp. 14–25, 2021.

[38] Y. Peng, A. Parsian, H. Khodadadi et al., "Develop optimal network topology of artificial neural network (AONN) to predict the hybrid nanofluids thermal conductivity according to the empirical data of Al2O3–Cu nanoparticles dispersed in ethylene glycol," *Physica A: Statistical Mechanics and Its Applications*, vol. 549, Article ID 124015, 2020.

[39] L. Li, Y. Zhai, Y. Jin, J. Wang, H. Wang, and M. Ma, "Stability, thermal performance and artificial neural network modeling of viscosity and thermal conductivity of Al2O3-ethylene glycol nanofluids," *Powder Technology*, vol. 363, pp. 360–368, 2020.

[40] A. B. Çolak, "Experimental study for thermal conductivity of water-based zirconium oxide nanofluid: developing optimal artificial neural network and proposing new correlation," *International Journal of Energy Research*, vol. 45, no. 2, pp. 2912–2930, 2021.

[41] S. D. Barewar, S. Tawri, and S. S. Chougule, "Experimental investigation of thermal conductivity and its ANN modeling for glycol-based Ag/ZnO hybrid nanofluids with low concentration," *Journal of Thermal Analysis and Calorimetry*, vol. 139, no. 3, pp. 1779–1790, 2020.

[42] M. Ghazvini, H. Maddah, R. Peymanfar, M. H. Ahmadi, and R. Kumar, "Experimental evaluation and artificial neural network modeling of thermal conductivity of water based nanofluid containing magnetic copper nanoparticles," *Physica A: Statistical Mechanics and Its Applications*, vol. 551, Article ID 124127, 2020.

[43] W. He, B. Ruhani, D. Toghraie et al., "Using of artificial neural networks (ANNs) to predict the thermal conductivity of zinc oxide–silver (50%–50%)/water hybrid Newtonian nanofluid," *International Communications in Heat and Mass Transfer*, vol. 116, Article ID 104645, 2020.

[44] A. Pare and S. K. Ghosh, "A unique thermal conductivity model (ANN) for nanofluid based on experimental study," *Powder Technology*, vol. 377, pp. 429–438, 2021.

[45] S. Rostami, A. A. Nadooshan, A. Raisi, and M. Bayareh, "Modeling the thermal conductivity ratio of an antifreeze-based hybrid nanofluid containing graphene oxide and copper oxide for using in thermal systems," *Journal of Materials Research and Technology*, vol. 11, pp. 2294–2304, 2021.

[46] C. J. Ho and J. Gao, "Preparation and thermophysical properties of nanoparticle-in-paraffin emulsion as phase change material," *International Communications in Heat and Mass Transfer*, vol. 36, no. 5, pp. 467–470, 2009.

[47] M. Taki, A. Rohani, F. Soheili-Fard, and A. Abdeshahi, "Assessment of energy consumption and modeling of output energy for wheat production by neural network (MLP and RBF) and Gaussian process regression (GPR) models," *Journal of Cleaner Production*, vol. 172, pp. 3028–3041, 2018.

[48] M. Jamei, I. Ahmadianfar, I. A. Olumegbon, M. Karbasi, and A. Asadi, "On the assessment of specific heat capacity of nanofluids for solar energy applications: application of Gaussian process regression (GPR) approach," *Journal of Energy Storage*, vol. 33, Article ID 102067, 2021.

[49] C. E. Rasmussen, "Gaussian processes in machine learning," in *Summer School on Machine Learning*, Springer, Berlin, Germany, 2003.

[50] J. Park, D. Lechevalier, R. Ak et al., "Gaussian process regression (GPR) representation in predictive model markup language (PMML)," *Smart and sustainable manufacturing systems*, vol. 1, no. 1, p. 121, 2017.

[51] X. Zhou, F. Zhou, and M. Naseri, "An insight into the estimation of frost thermal conductivity on parallel surface channels using kernel based GPR strategy," *Scientific Reports*, vol. 11, no. 1, pp. 7203–7211, 2021.

[52] M. Mahdaviara, A. Rostami, F. Keivanimehr, and K. Shahbazi, "Accurate determination of permeability in carbonate reservoirs using Gaussian Process Regression," *Journal of Petroleum Science and Engineering*, vol. 196, Article ID 107807, 2021.

[53] B. Wang and I. Alruyemi, "Comprehensive modeling in predicting biodiesel density using Gaussian process regression approach," *BioMed Research International*, vol. 2021, Article ID 6069010, 13 pages, 2021.

[54] S. Inyurt, M. Hasanpour Kashani, and A. Sekertekin, "Ionospheric TEC forecasting using Gaussian process regression (GPR) and multiple linear regression (MLR) in Turkey," *Astrophysics and Space Science*, vol. 365, no. 6, pp. 99–17, 2020.

[55] S. Wang, W. Li, and I. Alruyemi, "On the investigation of effective factors on higher heating value of biodiesel: robust modeling and data assessments," *BioMed Research International*, vol. 2021, Article ID 4814888, 9 pages, 2021.

[56] N. Nabipour, S. N. Qasem, A. Mosavi, and S. Shamshirband, *Gaussian Process Prediction Model to Estimate Excess Adsorption Capacity of Supercritical CO_2*, Preprints, 2020.

[57] J. Wang and J. Hu, "A robust combination approach for short-term wind speed forecasting and analysis–combination of the ARIMA (autoregressive integrated moving average), ELM (extreme learning machine), SVM (support vector machine) and LSSVM (least square SVM) forecasts using a GPR (Gaussian process regression) model," *Energy*, vol. 93, pp. 41–56, 2015.

[58] Q. Wu, R. Law, and X. Xu, "A sparse Gaussian process regression model for tourism demand forecasting in Hong Kong," *Expert Systems with Applications*, vol. 39, no. 5, pp. 4769–4774, 2012.

[59] A. R. Ghanizadeh, N. Heidarabadizadeh, and F. Heravi, "Gaussian process regression (Gpr) for auto-estimation of resilient modulus of stabilized base materials," *Journal of Soft Computing in Civil Engineering*, vol. 5, no. 1, pp. 80–94, 2021.

[60] F. Mousazadeh, M. H. T. Naeem, R. Daneshfar, B. S. Soulgani, and M. Naseri, "Predicting the condensate viscosity near the wellbore by ELM and ANFIS-PSO strategies," *Journal of Petroleum Science and Engineering*, vol. 204, Article ID 108708, 2021.

[61] D. Ahangari, R. Daneshfar, M. Zakeri, S. Ashoori, and B. S. Soulgani, "On the prediction of geochemical parameters (TOC, S1 and S2) by considering well log parameters using ANFIS and LSSVM strategies," *Petroleum*, 2021.

[62] A. Bemani, Q. Xiong, A. Baghban, S. Habibzadeh, A. H. Mohammadi, and M. H. Doranehgard, "Modeling of cetane number of biodiesel from fatty acid methyl ester (FAME) information using GA-PSO-and HGAPSO-LSSVM models," *Renewable Energy*, vol. 150, pp. 924–934, 2020.

[63] R. Razavi, A. Bemani, A. Baghban, A. H. Mohammadi, and S. Habibzadeh, "An insight into the estimation of fatty acid methyl ester based biodiesel properties using a LSSVM model," *Fuel*, vol. 243, pp. 133–141, 2019.

[64] R. Razavi, A. Sabaghmoghadam, A. Bemani, A. Baghban, Kw Chau, and E. Salwana, "Application of ANFIS and LSSVM strategies for estimating thermal conductivity enhancement of metal and metal oxide based nanofluids," *Engineering Applications of Computational Fluid Mechanics*, vol. 13, no. 1, pp. 560–578, 2019.

[65] A. Bemani, A. Baghban, A. H. Mohammadi, and P. O. Andersen, "Estimation of adsorption capacity of CO2, CH4, and their binary mixtures in Quidam shale using LSSVM: application in CO2 enhanced shale gas recovery and CO2 storage," *Journal of Natural Gas Science and Engineering*, vol. 76, Article ID 103204, 2020.

[66] A. Bemani, A. Baghban, and A. H. Mohammadi, "An insight into the modeling of sulfur content of sour gases in

supercritical region," *Journal of Petroleum Science and Engineering*, vol. 184, Article ID 106459, 2020.

[67] R. Setiawan, R. Daneshfar, O. Rezvanjou, S. Ashoori, and M. Naseri, "Surface tension of binary mixtures containing environmentally friendly ionic liquids: insights from artificial intelligence," *Environment, Development and Sustainability*, vol. 23, no. 12, pp. 17606–17627, 2021.

[68] S. M. Alizadeh, I. Alruyemi, R. Daneshfar, M. Mohammadi-Khanaposhtani, and M. Naseri, "An insight into the estimation of drilling fluid density at HPHT condition using PSO-ICA-and GA-LSSVM strategies," *Scientific Reports*, vol. 11, no. 1, pp. 1–14, 2021.